LHCb Collaboration LHCb 2004-052 VELO
30 June, 2004

Results from the First Test Beam of a Large Microstrip Czochralski Silicon Detector Equipped with LHC Speed Electronics

A Bates[a,b], J Buytaert[a], P Collins[a], D Eckstein[a], J Kennedy[b], T Ketel[d], J Palacios[c], C Parkes[b], U Parzefall[a], I Stavitski[c], N Tuning [a]

[a] CERN, CH-1211, Geneva 23, Switzerland.

[b] The University of Glasgow, Dept. of Physics and Astronomy, Glasgow, G12 8QQ.

[c] University of Liverpool, Oliver Lodge Laboratory, Oxford Street, Liverpool, L69 7ZF, UK.

[d] NIKHEF, Kruislaan 409, 1098 SJ Amsterdam, The Netherlands.

Abstract

The first charge collection efficiency and signal to noise studies of a 6 x 4 cm microstrip Czochralski silicon detector are presented. The detector was read out with LHC speed electronics with the aim of evaluating its performance for the LHCb VELO upgrade. The charge collection efficiency distribution as a function of voltage showed detector depletion at 550 V. A minimum lower bound for the signal to noise ratio was measured as 23.5±2.5 for this 50 μm pitch 380 μm thick detector. The detector was then irradiated inhomogeneously and the performance studies repeated as a function of irradiation. The results were promising; signal to noise ratio values of 17, 11 and 7 for 0.5, 2 and 4 equivalent years of the maximum LHCb radiation ($1\text{x}10^{14}$ 1 MeV neuton equivalent cm^{-2}) respectively. The effect of the voltage on the signal to noise ratio was also investigated.

1 Introduction

This note presents the results of a test-beam study of an irradiated micro-strip Czochralski (Cz) silicon sensor. Section 1 provides an introduction to the expected radiation hardness properties of Cz silicon and its potential importance for the LHCb experiment. Section 2 describes the Czochralski detector used in these studies. The detector was tested in a 120 GeV pion and muon CERN SPS testbeam before irradition in the autumn of 2002 and post-irradiation in summer 2003. The irradiation was performed with 24 GeV protons in the CERN PS as descibed in section 3. Section 3 also provides simulation results. The set of silicon sensors, known as the VELO telescope, used to track the testbeam particles is described in section 4. In section 5 the procedure that was used to select data for analysis is presented. This involved alignment and event selection cuts. The charge collection efficiency and signal to noise performance of the first microstrip Cz detector read out at LHC speed clocking rates will be presented in sections 6 and 7 respectively.

1.1 Czochralski Silicon

There are two methods of mono-crystalline silicon growth: the Float Zone (FZ) method and the Czochralski (Cz) technique. The FZ method can yield high purity and high resistivity silicon suitable for high energy particle physics tracking and detection. It is this material that has been used in the harsh radiation environments of HEP experiments. Silicon produced using the Cz method is generally of lower resistivity, as low as 1-2 mΩcm[1] which makes it very useful for IC technology but not suitable for microstrip or pixel detectors. The Cz method involves the controlled pulling of a mono-crystalline ingot out of a rotating crucible containing a melt of polycrystalline silicon. The process is carried out in an inert argon atmosphere to prevent the formation of SiC or SiO_2. The molten solution in the crucible is electrically conductive, hence the presence of a magnetic field can influence the flow properties of the melt. The relationship between magnetic field strength and temperature oscillations of the melt has been explored [1]. Developments in the Cz method such as these have lead to the possibility of high resistivity (1 kΩcm) detector grade MCz (Magnetic Czochralski) silicon.

The resistivity of Cz-silicon is limited by the diffusion of the impurities from the crucible into the molten silicon. The most important impurities are oxygen, carbon and boron. It is possible to control the oxygen concentration of the silicon through, for example, the melt flow rate and the rate of evaporation of oxygen from the surface of the melt [2]. The concentration of oxygen in silicon is an important parameter for silicon detectors. The relative performance of oxygenated FZ silicon detectors compared to standard FZ silicon has been investigated by the ROSE collaboration [3]. It was shown that the radiation hardness of FZ silicon when exposed to a charged hadron flux can be increased with elevated oxygenation concentrations, DOFZ (Diffusion Oxygenated Float Zone).

Since the work of the ROSE collaboration, it has been shown that ^{60}Co γ irradiation of FZ silicon creates deep acceptor defects which may be described as a cluster of 2 vacancies and an oxygen atom (V_2O). These deep levels can act as traps to charge created by radiation passing through silicon detectors. It has been shown that the formation of

[1]Topsil Semiconductor Materials A/S, Linderupvej 4, DK - 3600 Frederikssund

these deep levels is suppressed with elevated oxygen levels, and instead shallow donors (called thermal donors) are formed [4]. Thermal donors may be removed from silicon by well understood heat processes. Cz silicon has a higher oxygen concentration compared to DOFZ silicon, hence, with reduced deep level formation and controllable shallow donor formation, it may be proposed that Cz silicon should offer increased radiation hardness. The oxygen introduced into the silicon lattice by the Cz growth will be introduced mainly as interstitial oxygen atoms (O_i), but also as dimers (O_{2i}). These dimers may also alter the radiation hardness of Cz material.

1.2 LHCb VELO Upgrade

There are many motivating factors which suggest that Cz silicon may offer increased radiation hardness for future HEP experiments. The VErtex LOcator (VELO) of the LHCb experiment[5] will sit as close as 7 mm to the LHC beam axis to enable precise vertexing. The silicon station closest to the interaction point will receive an annual fluence of approximately $10^{14}/\text{cm}^2$ (1 MeV neutron equivalence) which will be dominated by charged hadrons. The VELO detector will operate in one of the most extreme radiation environments of any LHC experiment detector. Currently the sensors will survive an estimated 3 years. After this the signal to noise ratio of the detector will exceed the specified lower limit. These first sensors will be made from DOFZ silicon. It is important for the VELO upgrade to test the performance of Cz-grown silicon. Even if the performance of Cz silicon is not vastly superior to DOFZ silicon, the number of manufacturers that would deal with Cz material is large compared with the few manufacturers that are willing to make DOFZ sensors.

2 Detector Description

2.1 Czochralski Silicon Sensor

The detector under investigation was processed from a 380 μm thick wafer that was cut from a MCz-grown ingot. The n type wafer was manufactured by Okmetric Oyj[2] by adding phosphorous dopants to the silicon melt. The original wafer had a resistivity of approximately 900 Ωcm, and after device processing the value measured was 1150 Ωcm. The 50 μm pitch p-implanted parallel strips are 6.159 cm in length and 10 μm in width. The strips were AC coupled through a 200 μm dielectric SiO_2 film. WN_x bias resistors[3] connnected the ends of each strip. The bias rail provided a path for the DC leakage current. The total area of the detector is 32.5 cm^2. Details of the processing and characterisation of the device can be found in reference [2]. The depletion voltage was found to be 420 V before exposure to radiation. A photograph of the Cz-detector, equipped with the read out electronics can be seen in Figure 1.

[2] 01510 Vantaa, Finland

[3] For 10 % < x < 45 % of nitrogen content in WN_x the resistance was typically 200 $\mu\Omega$cm

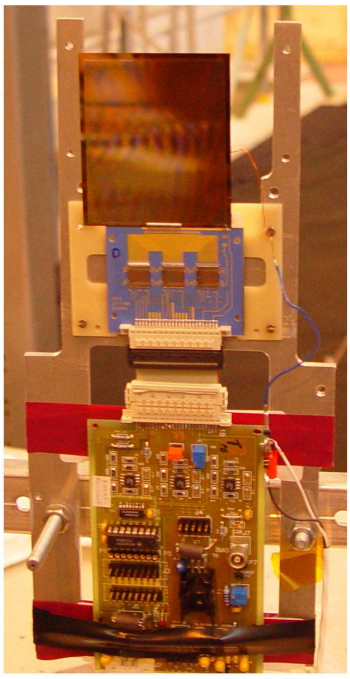

Figure 1: The Czochralski Silicon Detector equipped with 3 SCT128A read out chips. Only 2 were used in the analysis.

2.2 Front End Electronics

The SCT128A analogue read outchip was used for reading out the Cz test detector. Three of these chips were bonded to the centre region of the detector, but only two were used in the analysis. The SCT128A chips had a 40MHz clocking rate and were read out at a rate of 5MHz.

3 Irradiation and Annealing

3.1 Irradiation

Between 20:13 on 22/05/03 and 15:45 on 23/05/03 the Cz detector was irradiated with 24 GeV protons in the CERN PS irradiation facility. Details of the facility can be found in reference [8]. The average beam fluence was measured at $4.5\text{x}10^{14}$ p/cm^{2}h. The irradiations were especially difficult because the detector was already bonded to the hybrid containing the electronics which meant that the dimensions of the detector were greater than the shuttle used to manoeuvre the samples to be irradiated into the PS beam. Additionally, it was required to expose the electronics to the minimum radiation. The detector received approximately uniform irradiation in the local y direction (perpendicular to the strips).

In order to evaluate the detector performance it was important to accurately measure the radiation profile along the strip axis (local x-direction). Five pieces of 8 x 8 mm square aluminium pieces were placed along the strip axis. Each piece had an approximate mass of 18 mg. The aluminium was replaced after 12 hours of the irradiation. The fluence

received by the aluminium pieces was measured using an NaI spectrometer with varying accuracy (between 7-30%) depending on the activity of the aluminium. The position of the aluminium pieces with respect to the detector was only known to within ±5 mm but this was later improved using the data (see section 5.2.2).

A beam profile function was then fitted to the fluences measured from the aluminium pieces. The form of this function was determined using a layer of radiation sensitive film which was placed in front of the detector during the irradiation. The extent of the discolouration of the film was assumed to be linear with the radiation. The film was analysed using a colour intensity map and can be seen in Figure 2.

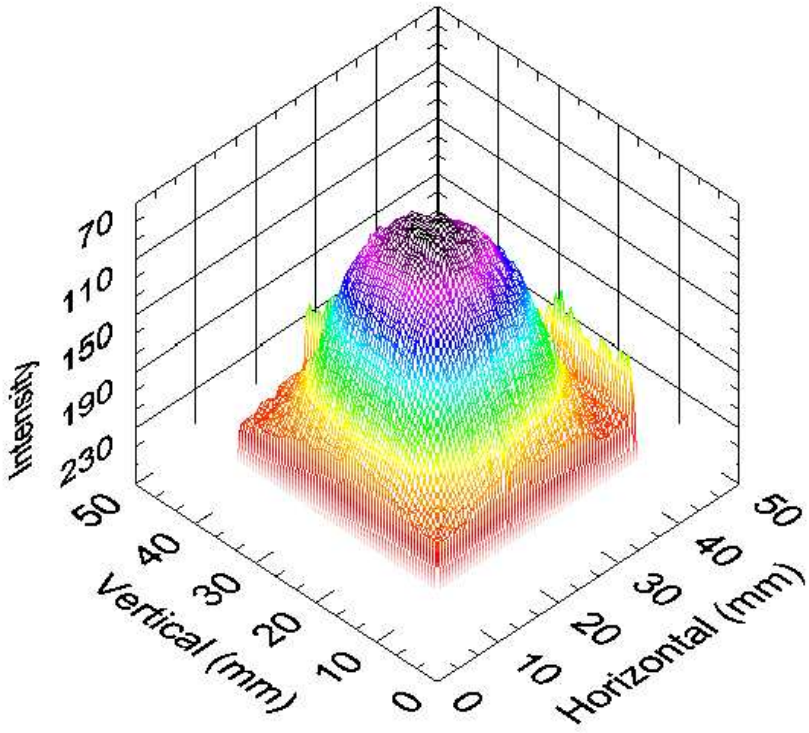

Figure 2: A colour intensity map of the radiation sensitive film that was exposed during the irradiation of the Cz detector. The vertical (horizontal) axis refers to the vertical (horizontal) side of the colour tape. The tape was perpendicular to the PS beam. The detector was placed approximately 175^o to the incoming PS beam.

Slices along the local x and y axes of the radiation sensitive film were plotted and can be seen in Figure 3. For each of these slices a Gaussian was fitted and found to agree well with the observed profile. Hence a Gaussian was fitted to the 5 measurements of the fluence from the aluminium, to produce the final beam profile experienced by each strip on the Cz detector, which can be seen in Figure 4. The χ^2/ndf of the fit was 0.29/2 and

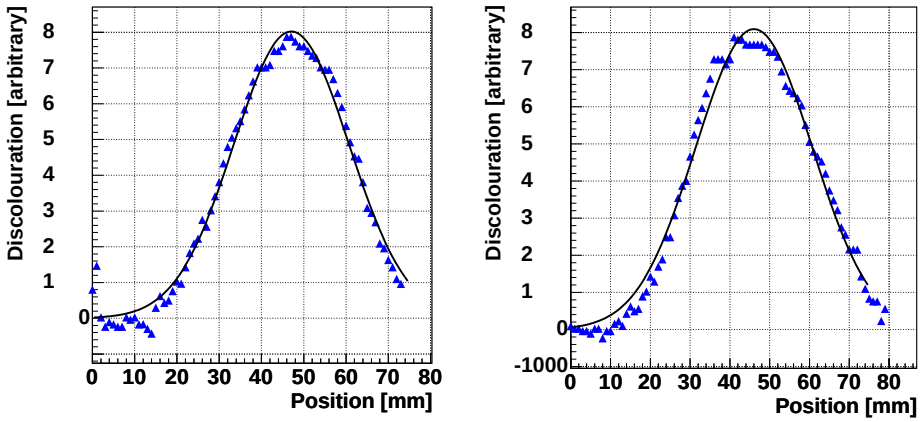

(a) (b)

Figure 3: Slices made through the 3D colour intensity map to sample the radiation profile: (a) x slice (b) y slice of the radiation sensitive film. See the text for discussion.

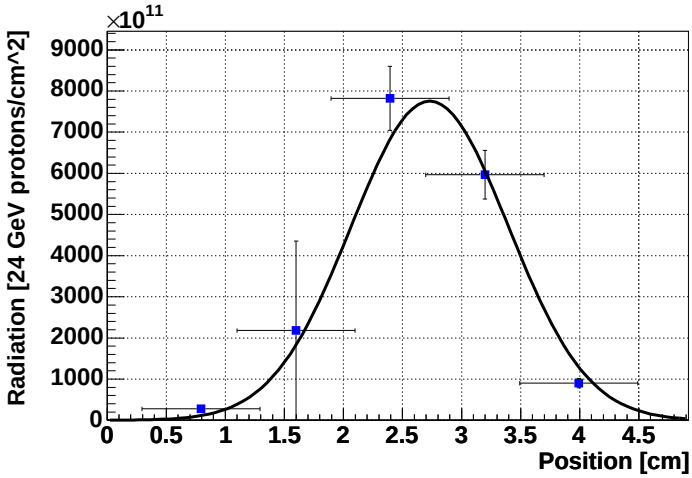

Figure 4: The points show the data measured from the aluminium pieces. The line show the result of a Gaussian fit.

the maximum radiation dose received was 7.8x10^{14} p/cm^2.

Figure 5 shows the outline of the Cz detector with the calculated radiation map superimposed.

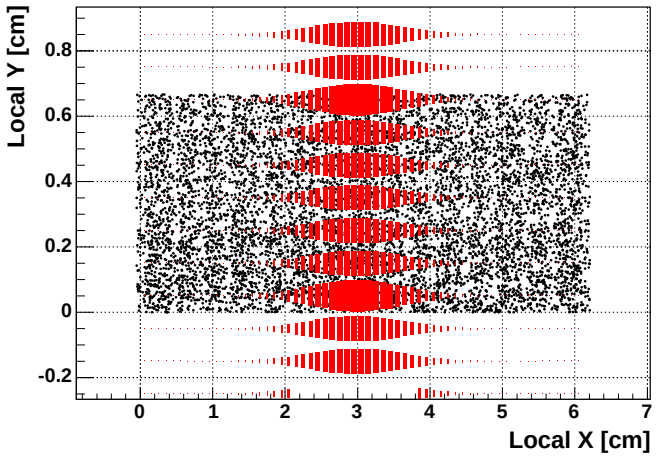

Figure 5: The black points shows the detector region. The strips run parallel to the local X axis. The superimposed red boxes shows the radiation received by each area of the detector. The size of the boxes is proportional to the received fluence. The irradiation was assumed to be uniform in the local Y direction. The irradiation was described by a Gaussian distribution along the X axis.

3.2 Annealing

The temperature of the detector was monitored during the irradiation procedure and prior to the collection of data in the test beam. The temperature of the detector during all periods where it was above 0^0C is shown in Figure 6(a). The detector was usually kept below -10^0C. A phenomenological parametrization of the bulk radiation damage to silicon has been developed by the Hamburg group of the ROSE Collaboration [9]. The model is based on experimental results from the study of silicon diodes. Parameter values are not yet available for Cz silicon, instead a simulation has been performed of a float zone silicon device. These results will permit an assessment of the relative performance of the Cz silicon device tested. Using this model, the evolution of the depletion voltage of a float zone device has been simulated and is shown in Figure 6 (b) for a range of fluences. The model parameter values were taken from [10]. During the irradiation period a sharp increase in the depletion voltage of the device is expected. This is followed by a period of beneficial annealing before the depletion voltage again starts to rise. Final depletion voltages of 1070 V, 650 V and 150 V are expected for the irradiation doses of 7 $\times$ 10^{14}, 4.25 $\times$ 10^{14} and 1.25 $\times$ 10^{14} 24 GeV protons /cm^2. The NIEL scaling factor to convert from 24 GeV protons to 1 MeV neutrons is 0.61.

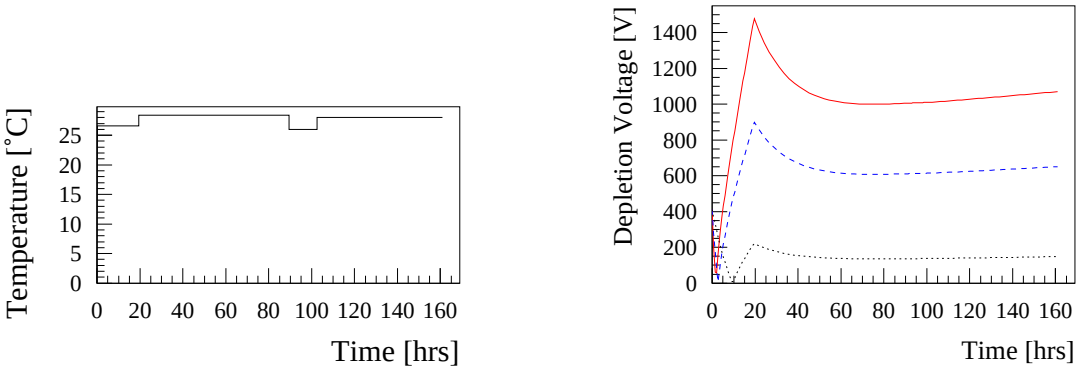

(a) (b)

Figure 6: The period that the detector spent above 0^0C during and after irradiation is shown in (a). The irradiation period was of 20 hours duration. The expected depletion voltage of a float zone silicon sensor is shown during the same period for a range of fluences in (b). The solid line corresponds to 7×10^{14}, the dashed line 4.25×10^{14} and the dotted line 1.25×10^{14} 24 GeV protons /cm^2.

The initial depletion voltage of a 380 micron thick float zone silicon sensor of 1150 Ω cm resistivity[4] is predicted as 410 V, which compares well with the measured value of 420 V. The final depletion voltage of the device, after type inversion, is predicted to be insensitive to the initial depletion voltage. The impact of measurement errors on the temperature and time profile for the period when the detector was not refrigerated give rise to an uncertainty on the peak fluence depletion voltage of around 50 V. The 10 % uncertainty on the peak irradiation fluence corresponds to a similar uncertainty on the depletion voltage. The model parameters have a significant variation between materials, changing individual parameters by the ranges reported in [10] and its references an uncertainty of around 200 V is obtained on the peak fluence simulation prediction. The model predicts a very significantly improved performance for diffusion oxygenated silicon over standard silicon under proton irradiation: under the same conditions the expected final depletion voltage of a diffusion oxygenated detector at maximum fluence would be around 350 V. In all the scenarios considered the final depletion voltage was found to lie in a fairly stable area on the reverse annealing slope just above the local minima of the curve.

4 Test Beam Set-up

4.1 Telescope

The setup used in the irradiated Cz test beam is illustrated in Figure 7. In 2002 the set up was similar. The detectors are all mounted on an optical bench and placed inside a light tight box, approximately 1 m in length. Tracks from 120 GeV pions and/or

[4]The initial resistivity of the wafer was 900 Ω cm rising to 1150 Ω cm after processing

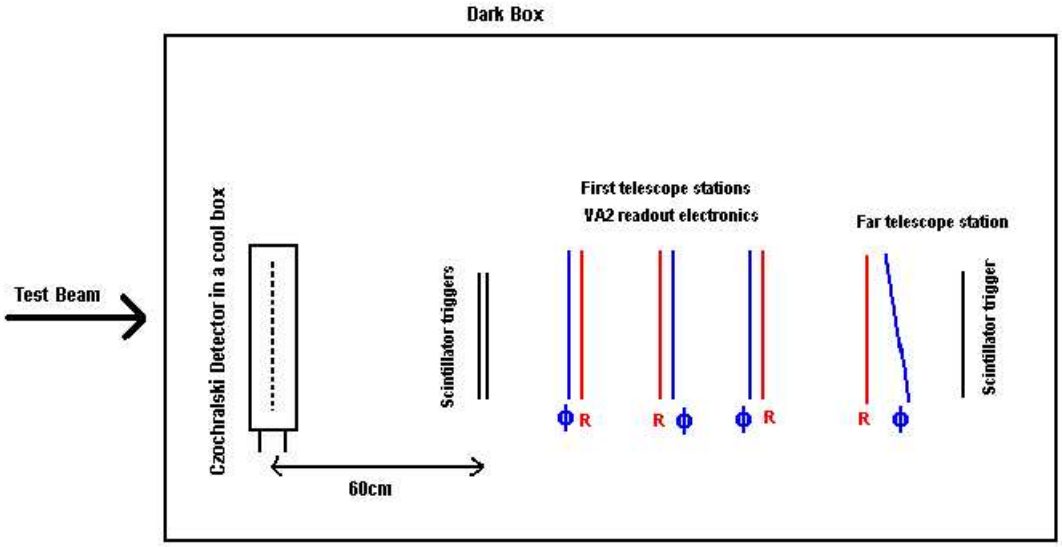

Figure 7: Schematic diagram of the VELO test beam set up in 2003. In the 2002 test beam set up the Cz detector was only 6 cm from the front of the first telescope stations.

muons are reconstructed using pairs of the first prototypes, PR01, of the VELO R and Phi sensors. These first sensors were manufactured by Hamamatsu Photonics[5] in 1998 and details are described in reference [11]. The telescope detectors were equipped with slow VA2 electronics. As can be seen in Figure 7, there are 3 pairs of sensors in the first telescope and 2 sensors in the far telescope. In the far stations the Φ sensor is inclined to optimize the detector resolution. Normally the detector under test would be placed in between the telescope and the far telescope, however, due to spatial constraints the Czochralski detector was placed before the telescope stations in both of the test beams. However, in the unirradiated testbeam the Cz detector was placed only 6 cm from the first telescope stations and not 60 cm as in the 2003 test beam, see Figure 7.

There were two large scintillators placed at the near and far sides of the telescope detectors. The scintillators were specially cut to match the telescope's fiducial area and produced a trigger signal if co-incident pulses occurred from both scintillators (accounting for spatial separation and non-equal cable lengths). The SCT128A chip used in the readout of the Cz detector, has an acceptance window which opens every 200 ns. In order to have the trigger acceptance window centered to the maximum of the chip pulse coming from the sensor, 1 ns adjustments could be made between the opening of the trigger acceptance window and the chip readout.

4.2 Test Station

In the 2003 testbeam, the Czochralski detector had been irradiated and annealed according to the simulations performed in section 3.2. Therefore, the detector was placed in a cool box which can be seen in Figure 8. The detector was mounted on an aluminium

[5]325-6, Sunayama-cho, Hamamatsu City, Shizoka Pref., 430-8587, Japan

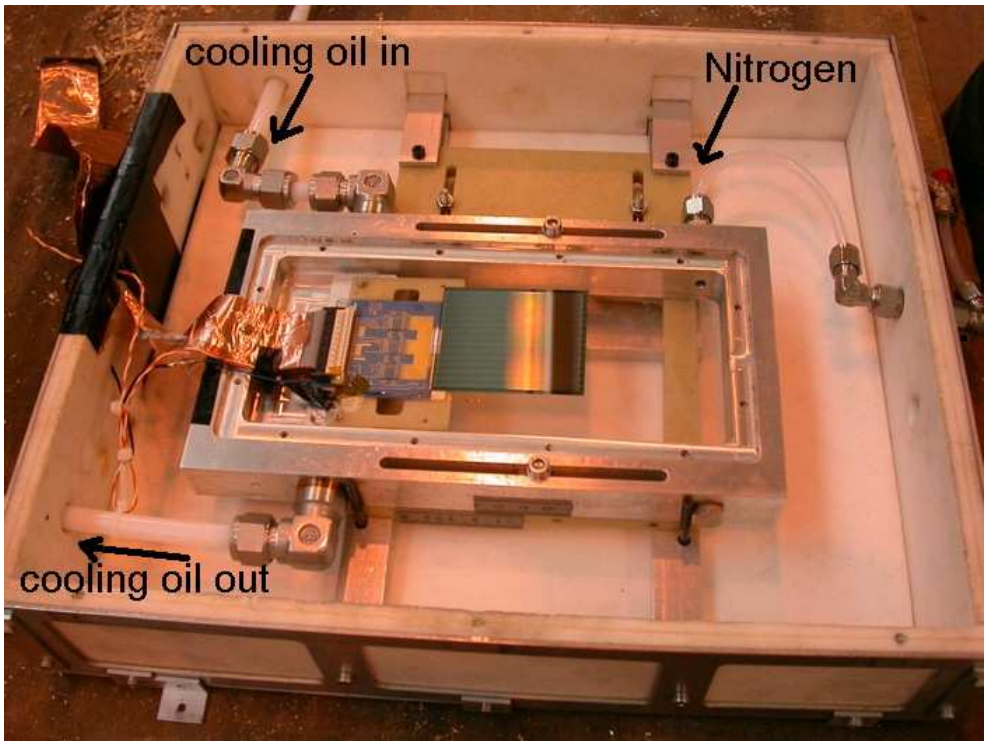

Figure 8: The cool box used to cool and support the Cz detector after irradiation. The silica cooling oil flowed through the aluminium base of the detector support. The detector was continually flushed with nitrogen.

plate which was cooled with silica oil and the detector was flushed with nitrogen. The temperature was monitored through a calibrated PT100 sensor. The approximate operating temperature was -10^{o}C. For the unirradiated Cz testbeam, no cooling was required and the test beam took place at room temperature.

5 Data Selection

5.1 Data

Data was collected at a range of different voltages. The data sets used in this analysis are described below. A typical data set contains 5000 events collected at the specified voltage.

- unirradiated Cz
  - 124 V, 350 V, 400 V, 500 V, 550 V, 700 V
- 1.25 x10^{14} protons/cm^2
  - 167 V, 243 V, 290 V, 371 V, 455 V
- 4.25 x10^{14} protons/cm^2
  - 167 V, 243 V, 290 V, 371 V
- 7.0 x10^{14} protons/cm^2
  - 167 V, 243 V, 290 V, 371 V

5.2 Alignment

The raw signal from the telescope detector strips had pedestal and common mode noise suppression algorithms applied. Clusters were then formed from the identified hits, subject to specified signal to noise ratio cuts for cluster formation. Tracks are fitted through the reconstructed telescope clusters [12]. The Cz detector was then aligned with respect to these reconstructed telescope tracks. The telescope track was then extrapolated to the Cz plane and a near-by Cz cluster is identified. The difference between the cluster centre and the sensor intercept point of the extrapolated telescope track is called the residual. Residuals, normalized to the uncertainty on the cluster position, are squared, summed and minimised for a given set of test beam tracks as a function of the 3 possible translational movements and the 3 possible rotational movements.

5.2.1 Non-irradiated Czochralski Data

The procedure described above was applied in order to achieve a satisfactory alignment to study the charge collection and signal to noise performance of the Cz detector prior to irradiation.

Asymmetric Charge Sharing During the 2002 test beam of the unirradiated Cz detector, some asymmetric charge sharing between the hit DAQ channel and the adjacent higher DAQ channel was observed. The origin of this problem has not been fully understood at the time of writing, but is thought it could be explained by some misalignment between the ADC and the chip timing. A correction was applied to the clustering routines that were used by the alignment procedure. The problem caused a larger than expected cluster width for the unirradiated data.

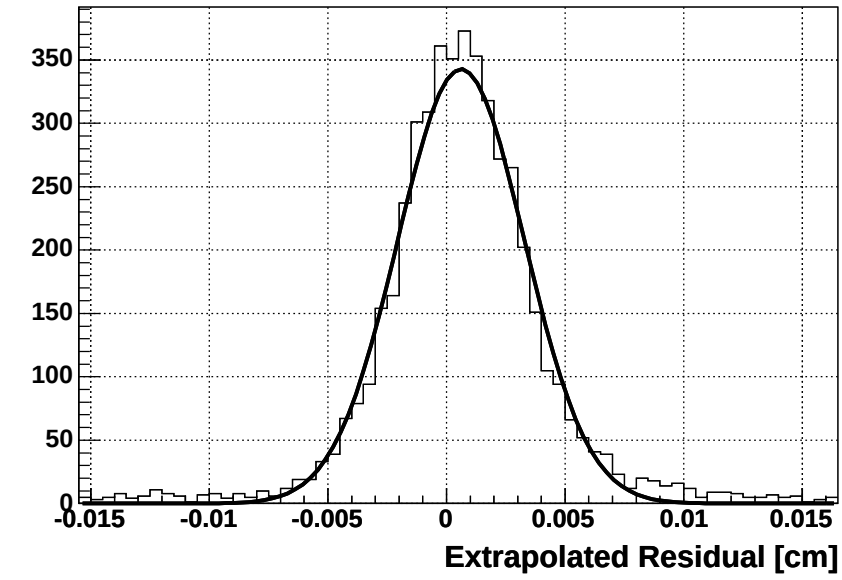

(a)

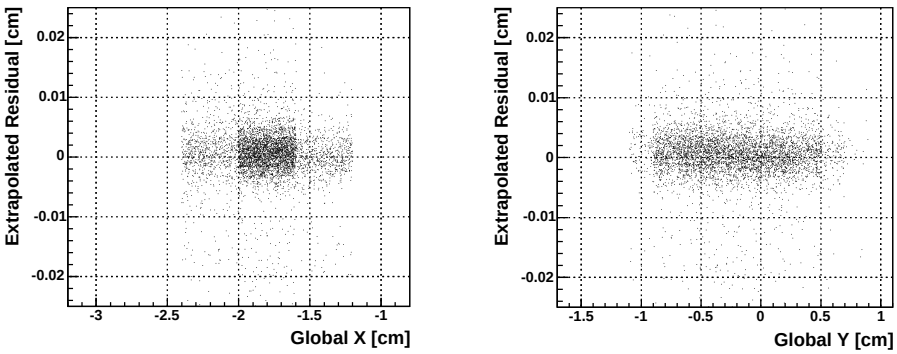

(b)

Figure 9: (a) The extrapolated residuals for the unirradiated Cz detector. The resolution of the fitted Gaussian yields a resolution of 26.7 μm $\pm$ 0.4μm (b) The extrapolated residual as a function of global x (left plot) and global y (right plot).

Resultant Alignment Figure 9 (a) shows the result of the alignment procedure on the unirradiated Cz data. The resolution of the detector is defined by the sigma of a Gaussian fit to the residuals. The resolution achieved was 26.7 μm $\pm$ 0.4 μm. The residuals show no dependence on x or y, as can be seen in Figure 9 (b). The alignment shown in these plots

was taken from a 500 V data run, but similar results (within ± 5 μm) can be achieved by applying the same alignment to the data taken at other voltages.

5.2.2 Irradiated Czochralski Data

The charge was plotted as a function of the local x of the detector and is shown in Figure 10 (a). This plot clearly shows the signal collected was lower in the regions of highest radiation exposure. The position of the minimum was found and was set to correspond to the maximum of the radiation profile found in Figure 10 (b). The irradiated data was split into 3 radiation bins along the strip direction and can be seen in Figure 10 (b). The average irradiation fluence from the bins was 7×10^{14}, 4.25×10^{14} and 1.25×10^{14} 24 GeV protons /cm^2.
Furthermore, the alignment was split into three separate alignments corresponding to

- 2-4 cm on the local x axis of the Cz detector which is the same region as the 2 highest radiation regions
- 0-2 cm on the local x axis of the Cz detector
- 4-6 cm on the local x axis of the Cz detector

The boundaries for the alignment regions were initially decided upon by using the first alignment file. Some tracks may be double counted at the boundaries between the alignment regions.

The final resolution calculated from the residuals for each alignment file can be seen in Figures 11 (a), (b) and (c). The resultant resolutions for each alignment were between 37 μm - 47 μm. Only one alignment resulted in spatial dependence, which is shown in Figure 11 (a). In this case the residual was only dependent on the y position of the track. This would have no effect on the irradiation bin that the track was included in since the irradiation was only a function of x. The variation is of the order ± 100 μm. The pitch of the detector is 50 μm, therefore from this effect alone at least ± 2 strips should be considered in the CCE and signal to noise ratio studies.

5.3 Event Selection

In order to detect very low charge, the raw test beam data had to be cleaned. The following cuts were applied in order to clean the data.

- Geometry
  For both Cz test beams, geometrical cuts were applied on the track extrapolation from the telescope to the Cz sensor. If the extrapolated track pointed outside the detector then these tracks were discarded.

- Dead, noisy and unbonded channels - 'masked' channels
  These were found from a visual inspection of the average noise of the strips and then the relevant strips were masked out from the analysis.
  Figure 12 shows the noise for the irradiated 2003 data before and after the common mode correction algorithm had been applied. The correction also implemented the mask of dead, noisy or unbonded strips. The same procedure was applied in the

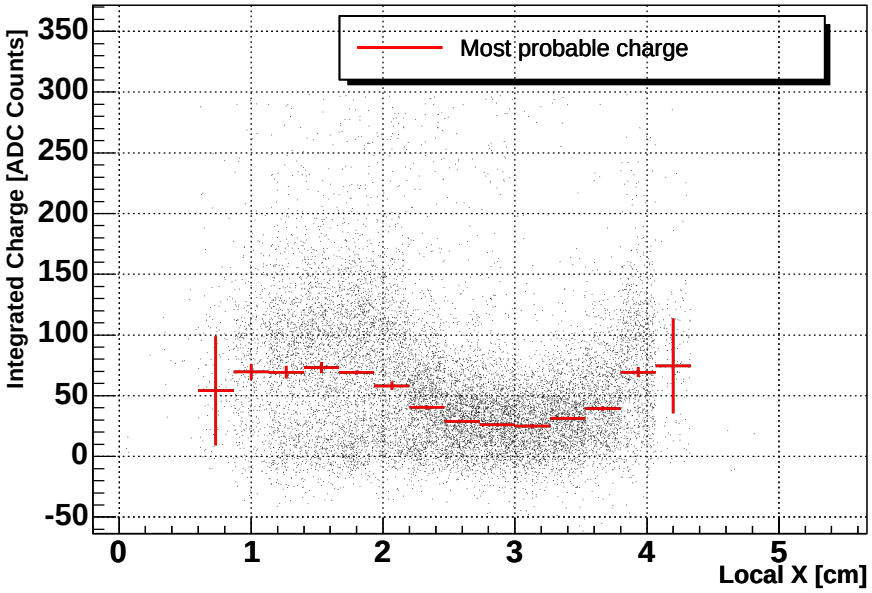

(a)

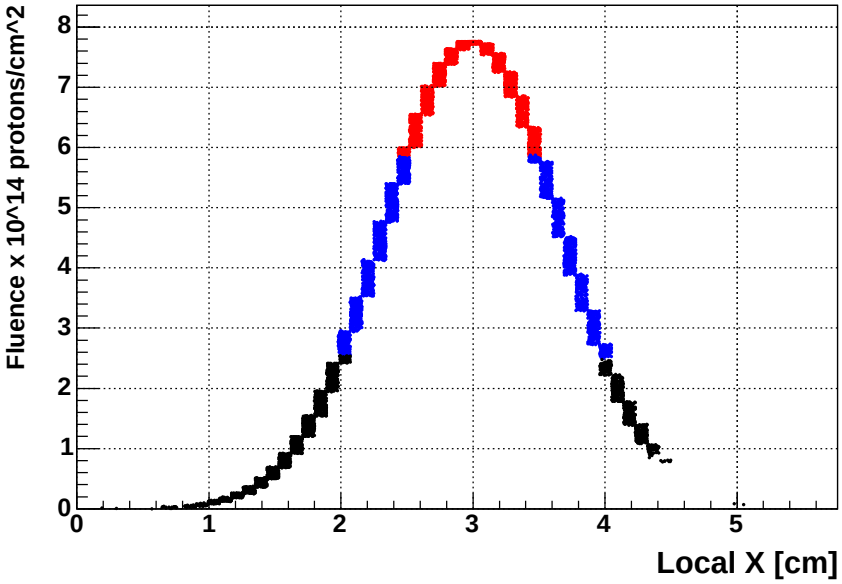

(b)

Figure 10: (a) Signal as function of the local x of the Czochralski detector. The signal loss due to radiation damage can be seen around 3 cm. The position of minimum charge collected is assumed to correspond to the position of maximum radiation damage. The most probable charge comes from fitting a landau convoluted with a Gaussian to each vertical slice of the integrated charge plot. (b) The minimum charge collected in (a) yields the position of maximum radiation damage. This dictates the placement of the radiation profile. The local x of the detector (along the strip axis) has been divided into 3 radiation bins. The local x positions between 2.5 and 3.5 cm (Red) corresponds to an average fluence of $7\text{x}10^{14}$ p/cm^2. The blue regions between 2 cm and 2.5 cm and 3.5 cm and 4 cm correspond to an average fluence of $4.25\text{x}10^{14}$ p/cm^2. The rest of the detector areas (black) average a fluence of $1.25\text{x}10^{14}$ p/cm^2.

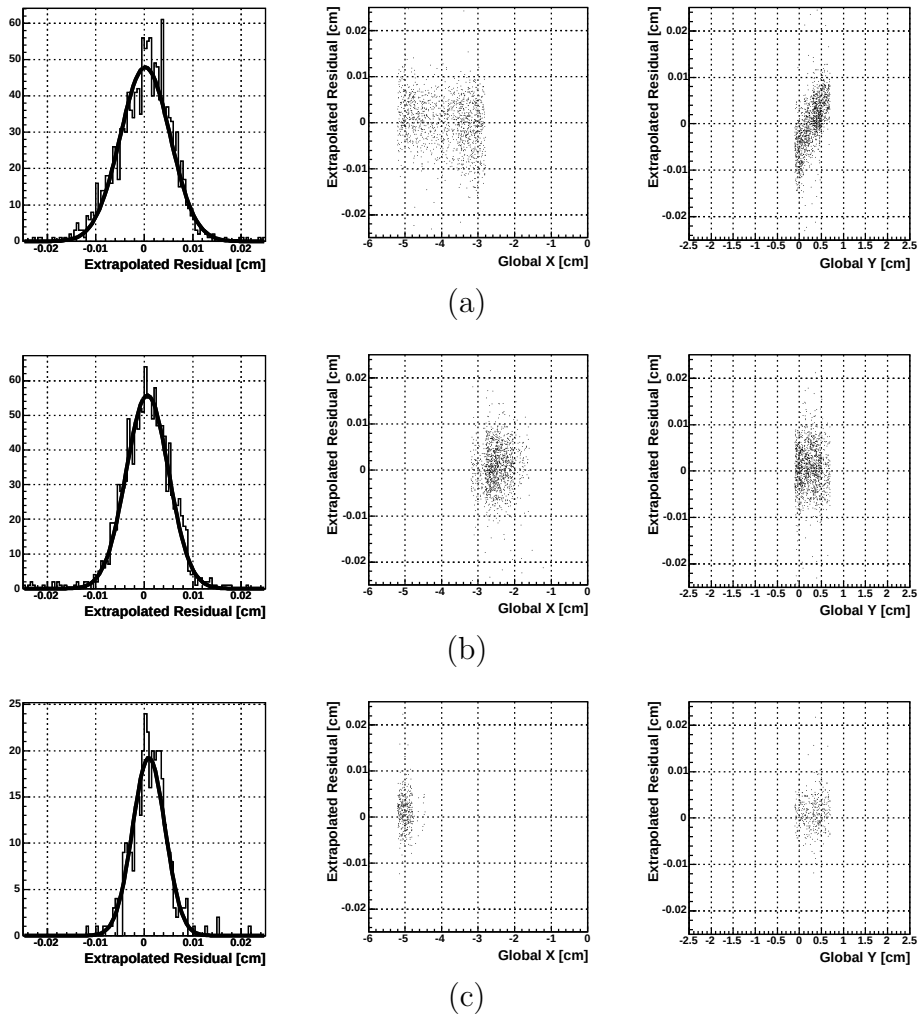

Figure 11: The alignment for the irradiated Cz detector (a) The extrapolated residuals for the first alignment area (consisting of the highest 2 irradiations areas) which yields a resolution of 47 μm. The centre plot shows the global x dependence and the right plots shows the global y dependence of the residuals. (b) The same plots for the second alignment region, which also has a resolution of 47 μm (c) The same plots for the second alignment region, which has a resolution of 37 μm.

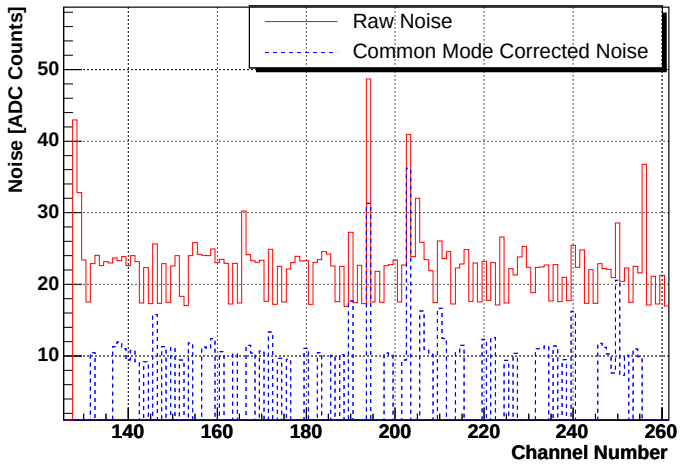

Figure 12: The noise for the irradiated Cz test beam. The solid line shows the raw noise for the channels on the chips of interest. The dashed line shows the noise after the common mode subtraction. The unbonded, noisy or dead strips have been masked out. These were determined from the strips performance over many data samples.

unirradiated Cz test beam where the number of dead, noisy or unbonded channels masked from the analysis was thirteen.

- No masked channels directly neighboring the strips of charge integration
  The region surrounding the intersection point between the Cz detector and the extrapolated telescope track should contain no masked strips. It was also required to not have any dead, noisy or unbonded strips directly neighbouring this region as can be seen in Figure 13. This cut resulted in a large reduction in the event statistics due to the large number of dead strips in the irradiated Cz beam test which can be seen in Figure 12.

- Timing cuts
  A very loose time window of 20 ns was applied in the irradiated Cz test beam. This timing cut defined the time interval when a track should arrive at the Cz sensor. This cut is sufficient for the analysis shown in these studies. For the unirradiated Cz data, a more stringent 10 ns window centred on the signal peak could be applied due to the better statistics.

- Tracks per event = 1
  The number of reconstructed tracks per event was specified to be one, so as to reject noise events where a track is picked which does not point to the Cz detector. 79% of events had only one track per event in the unirradiated testbeam and for the irradiated testbeam, 80% had one track per event, as can be seen in Figure 14.

The effects of these cuts can be seen in Figure 15 (a) and (b) for the unirradiated and irradiated pulse shapes respectively.

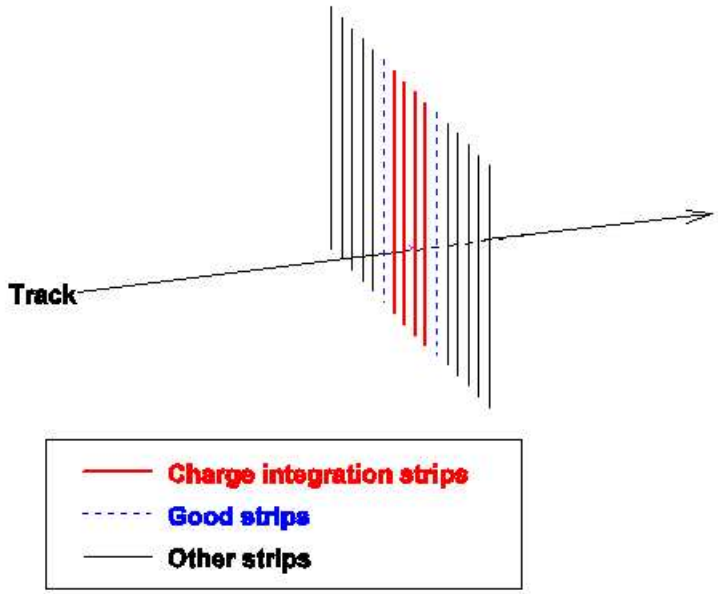

Figure 13: The reconstructed tracks from the telescope are extrapolated to the Cz detector. The four strips surrounding the point where the extrapolated track intercepts the detector (thick red lines) have their charge added. Any events which have dead, noisy, or unbonded strips inside the 4 strips or directly neighbouring the 4 strips are removed from the analysis.

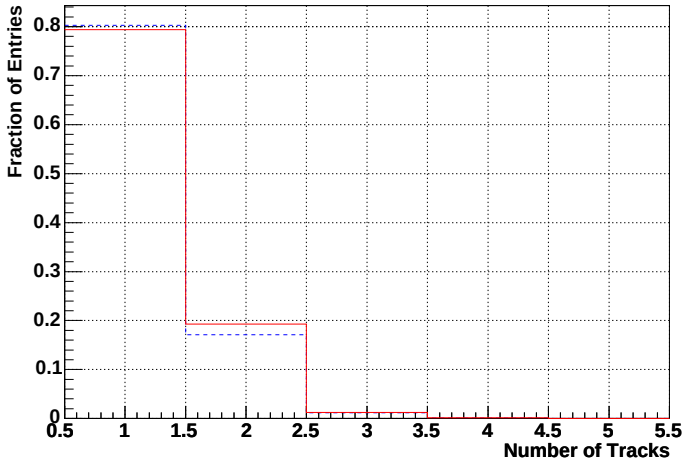

Figure 14: The number of tracks per event as a percentage. 79% of events had 1 track per entry in 2003 (red solid line) and 80% of events had 1 track per entry in 2002 (blue dashed line).

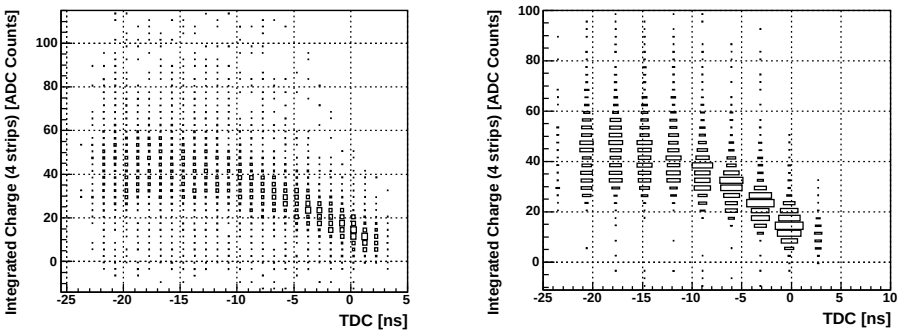

(a)

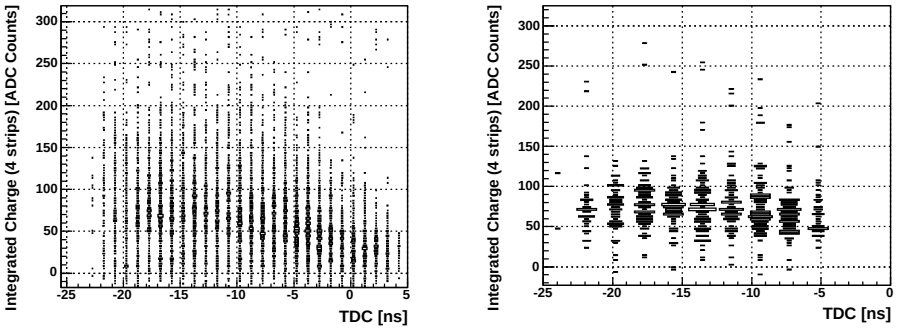

(b)

Figure 15: (a) 2002 unirradiated Cz test beam pulse shape before and after cleaning cuts (the time window shown here is for 25 ns but for the charge analysis only a 10 ns window was used between -20 ns to -10 ns). The 50% reduction in statistics before and after the cuts can be seen. (b) 2003 irradiated Cz test beam pulse shape before and after the cleaning cuts. Just the highest irradiation region is show as an example. The statistics after the cuts was so reduced, an alternative plotting mode was implemented. The charge is proportional to the box size.

6 Charge Collection Efficiency

6.1 Charge Integration

The charge was integrated over ±2 strips of the intersection point of the extrapolated track and the Cz detector. This choice was based on a number of issues. For both test beams the alignment was known better than 50 μm, which was the dimension of the strip pitch.

As described in section 5.2.1, in the 2002 test beam there was a problem of asymmetric charge sharing to a higher DAQ channel. This effect gave rise to a higher than expected cluster width. The average number of strips in an event was 3.3 strips. If this is coupled with the resoultion acheived for the uniradiated Cz test beam, the result is the charge collected in ±2 strips of the intersection point would not be the entire charge of the cluster. However, due to statistics, the charge will only be summed over ±2 strips of the intersection point. The cluster size was found to be independent of bias voltage applied, hence the shape of the charge collection as a function of voltage would not be altered.

In the 2003 test beam, one alignment configuration resulted in a y dependence of the residual to the extent of ±2 strips, see Figure 11 (a).

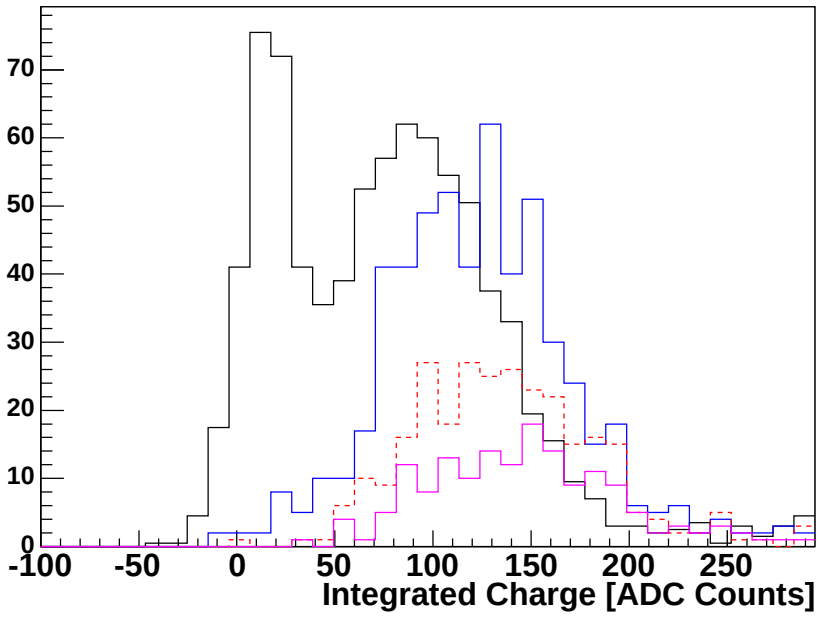

Figure 16: The integrated charge for a 290 V bias run and 4.25x10 ^{14}p/cm^2 run taken in the 2003 test beam period as a function of the integration strip width. Black = ±1 strip, blue = ±2 strips, red (dashed) = ±3 strips and purple = ±4 strips. See text for explanation.

Figure 16 shows the charge collected in the irradiated Cz testbeam as a function of the number of strips over which the integration was performed. The Gaussian distribution

centred on zero is from the noise. The noise contribution is significantly smaller for ±2 strips (4 strips in Figure 16) than for ±1 strips (2 strips in Figure 16).

When the region is 4 strips wide one can see that most of the charge is collected when compared to 6 or 8 strips wide. Hence for calculating the charge collection efficiency, the charge was integrated over ±2 strips around the intersection point.

6.2 Fit

A Landau convoluted with a Gaussian was fitted to the charge integrated over four strips and the most probable signal was evaluated from the fitted function. Equation 1 shows the function used in the fit.

$$f(x; x_{MP}, \sigma_G, \sigma_L) = \frac{1}{\sqrt{2\pi}} \frac{1}{\sigma_G \sigma_L} A \int f_L(x, x_{MP}, \sigma_L) f_G(x - x', \sigma_G) dx' \qquad (1)$$

σ_L and σ_G are the Landau and Gaussian distribution widths. A is the normalisation for the total area. x_{MP} is the most probable value of the Landau distribution. The integral was approximated by a sum over 400 steps between the integration limits of $x_o \pm 5\sigma_G$. The four fit parameters were σ_L, σ_G, A and x_{MP}. The Landau was taken from reference [13].

6.3 Results

The CCE was measured both as a function of irradiation and voltage. The CCE results for the unirradiated Cz are shown in Figure 17(a). The depletion voltage measured after detector fabrication was 420 V. The voltage at which the full charge is collected, is estimated to be in the region of 550 V.

The signal was measured in ADC counts. The unirradiated and irradiated Cz beam tests were conducted in separate periods hence the ADC settings differed and cannot be directly compared. The most probable signal as a function of voltage and irradiation can be seen in Figure 17(b). Unfortunately all the data available for the irradiated Cz test beam was for voltages less than 500 V. This was due to inadequate cooling, leading to thermal runaway within the Cz silicon. However, the marked effect of radiation on the under-depleted silicon can be seen in Figure 17(b). For the area with the lowest radiation exposure the charge collected appears to start to level at voltages above 300 V. The annealing simulation performed for FZ grown silicon resulted in the full depletion voltage for this lowest radiation region to be 150 V, see Section 3.2. Hence, the least irradiated region was operated above its full depletion voltage.

Note, that due to charge trapping effects, it may be necessary to significantly over-deplete an irradiated detector before the full charge is collected. The asymmetric charge sharing problem described in sections 5.2.1 and 6.1 also leads to the full charge not being collected in the uniradiated Cz detector. The fraction of charge lost has been shown to be independent of voltage, hence this leaves the shape of the curve unchanged.

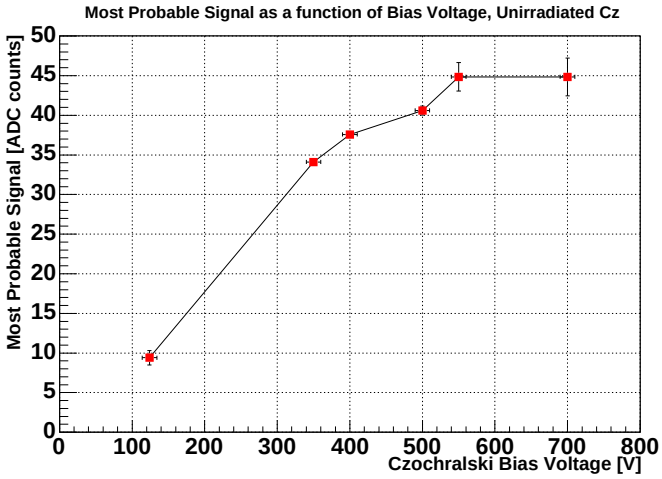

(a)

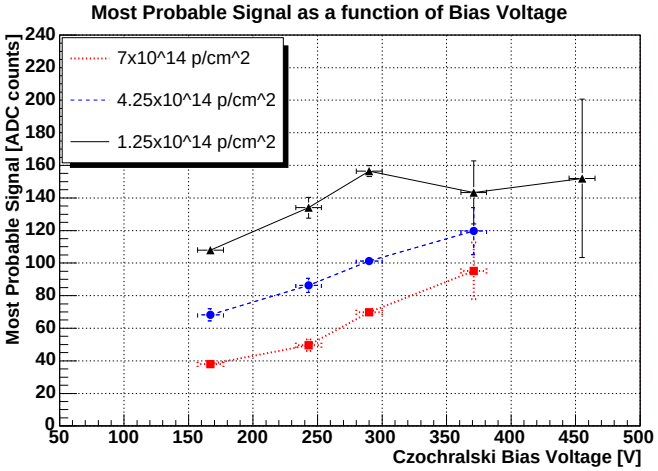

(b)

Figure 17: (a)Unirradiated CCE for the Czochralski silicon detector. (b) The CCE for the irradiated Cz detector. The radiation levels are quoted for 24 GeV protons/cm^2. The ADC values in the unirradiated and irradiated test beam periods can not be directly compared.

7 Signal to Noise Ratio Measurement

7.1 Unirradiated Czochralski Detector

The signal as a function of time for the unirradiated Cz detector was shown in Figure 15 (a). For each time slice a function was fitted which was described by a Landau convoluted with a Gaussian, see section 6.2. This function accurately describes the shape of the collected charge. The tail of the signal pulse is described by a Gaussian function and the convoluted function fitted gives a good agreement for this condition. It also agrees well with the time slice in the peak signal region, where a Landau fit bests describes the distribution. The fit results can be seen in Figure 18 (a).

Figure 18 (b) shows the most probable signal from the fits plotted as a function of time, superimposed on the unfitted pulse shape. The time was measured in ns but the 0 ns time held no significance. This analysis was repeated for data collected at a range of voltages and the peak shapes can be seen in Figure 19.

The noise level is estimated by taking the average noise value, after applying a common mode subtraction, for the four strips used to estimate the signal. The signal to noise ratio is defined as the ratio of the integrated signal to this average noise value. The signal to noise ratio for the unirradiated 380 μm detector can be seen for various voltages in Figure 20. The peak signal to noise ratio is approximately 23.5 $\pm$ 2.5 for this large p-on-n unirradiated Cz detector. In the VELO Technical Design Report, it is stated that the VELO aims to have a starting signal to noise ratio of more than 14 [5] for 220 μm thick detectors. The signal to noise ratio from the 380 μm Cz can be scaled to an equivalent value for a 220 μm Cz detector of 13.6 $\pm$ 1.5, assuming the noise is independent of the sensor thickness. The asymetric charge sharing problem, described in sections 5.2.1 and 6.1, resulted in the charge integrated around the intersection of the particle track and detector, was underestimated. The signal to noise value of 23.5 $\pm$ 2.5 is correct for the charge summed over $\pm$ 2 strips around the intersection point of the track. However, this was not all the charge hence the value of 23.5 is conservative and provides a lower bound for the pre-irradiated Cz signal to noise.

7.2 Irradiated Czochralski Detector

The same technique was applied to each of the three radiation levels with the 2003 irradiated Cz test beam. The mean signal as a function of voltage was found for each radiation and voltage sample as stated in Section 5.1. The quality of the Landau-Gaussian fits was poorer than on the unirradiated Cz data due to the lack of statistics. An example of the signal shape fit is shown in Figure 21. Although the features of the pulse shape could not be resolved from the fits, the quality was high enough to provide a measure of the signal to noise ratio for the irradiated Cz as a function of irradiation. Figure 22 shows the signal to noise ratio for the Cz detector at 3 levels of radiation damage. After approximately 6 months of the sensor being exposed to the LHCb radiation environment, the signal to noise ratio has been measured as 15. Figure 23 shows the signal to noise values measured for the 1.25×10^{14} 24 GeV p/cm^2 radiation area for 243 V and 290 V. Both of these voltages are above the full depletion voltage of the detector but the effect of 47 V of bias has moved the measured signal to noise ratio from 15 to 11.5. This shows the sensitivity

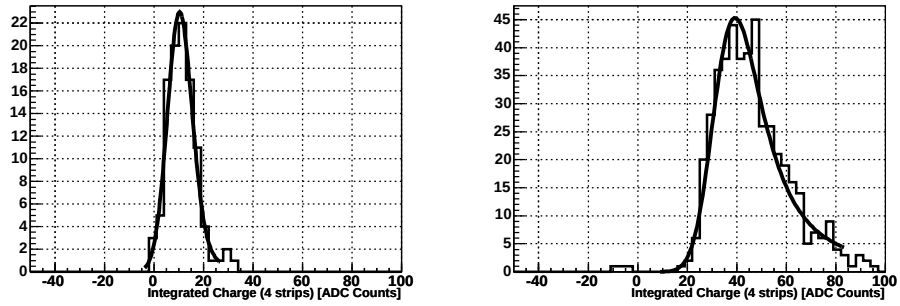

(a)

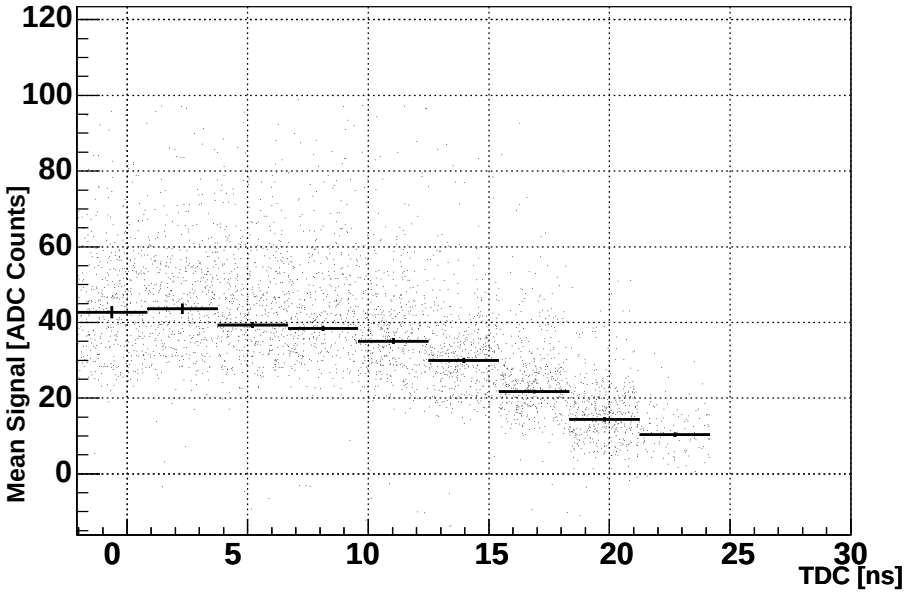

(b)

Figure 18: (a) Example fits from the function described by a Landau convoluted with a Gaussian. The left figure is from the tail of the signal and is described as a Gaussian. The figure on the right is an example fit from the peak region which is best described by a Landau function. The Landau-Gaussian fit performs well for both of the extreme conditions. (b) The signal as a function of time for a 500V unirradiated Cz sample. The Landau-Gaussian fit results for each time bin is superimposed. The time scale is arbitrary.

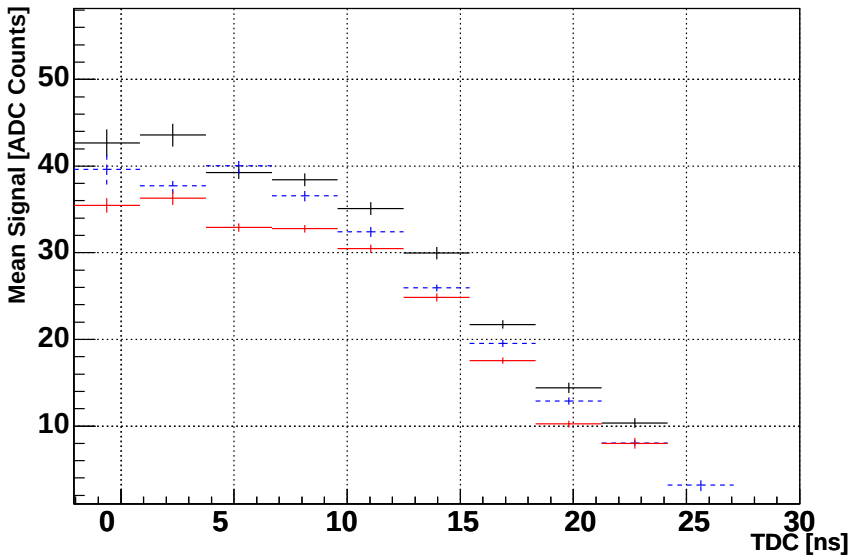

Figure 19: Signal pulses for 500 V (solid black points), 400 V (blue dotted points) and 350 V (red solid points). The mean signal is lower for lower voltages due to increased under-depletion.

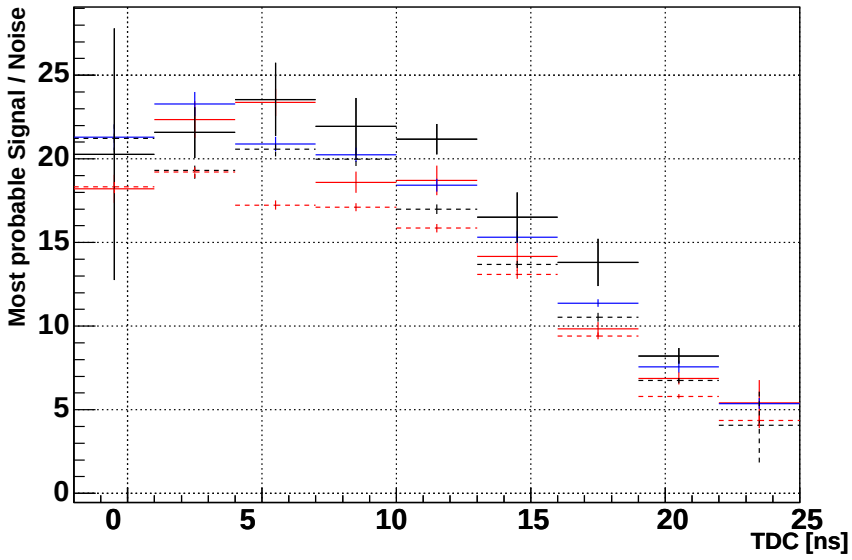

Figure 20: Signal to noise ratio for unirradiated Cz detector. 700 V (black solid points), 550 V (red solid points), 500 V (blue solid points), 400 V (black dashed points) , 350 V (red dashed points). The peak signal to noise ratio is estimated at 23.5 $\pm$ 2.5.

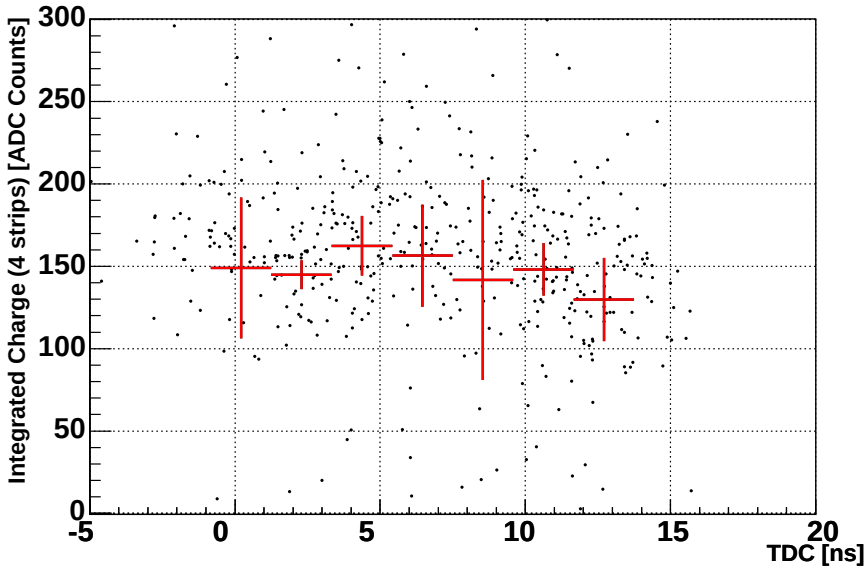

Figure 21: Mean signal measured for 290 V bias on the Cz detector and in an area which was exposed to an average of 1.25x10^{14} p/cm^2. Due to very limited statistics, the peak signal and trailing edge can not be resolved.

of the signal to noise ratio upon the voltage.

8 Conclusions

The first large p-on-n microstrip Czochralski silicon detector equipped with LHC speed electronics was assessed before and after irradiation in successful beam tests with 120 GeV muons and pions. Before irradiation the 380 μm thick detector gave a signal to noise ratio of 23.5 $\pm$ 2.5, which serves as a lower bound for the signal to noise ratio. After its manufacture the detector was measured to deplete at 420 V. Before irradiation the mean signal as a function of voltage was evaluated and the depletion voltage was determined as approximately 550 V. In the VELO Technical Design Report, it is stated that the VELO aims to have a starting signal to noise ratio of more than 14 for 220 μm thick detectors. The signal to noise ratio from the 380 μm Cz can be scaled to an equivalent value for a 220 μm Cz detector of 13.6 $\pm$ 1.5, assuming the noise remains constant.

The detector was then successfully irradiated with 24 GeV protons in the CERN PS facility. After harsh radiation exposure equivalent to 0.5, 2 and 4 years of the peak VELO LHCb radiation environment, the Czochralski detector survived and gave some promising results. The charge collection as a function of voltage was found and evidence of depletion was seen for the lowest radiation area. Signal to noise values of 15, 11 and 7 were found for radiation regions equivalent to 0.5, 2 and 4 years of the LHCb radiation environment, respectively, when the Cz was under-depleted for the highest 2 radiation regions. The effect of a 50 V increase on the irradiated Cz detector was also seen to strongly influence the signal to noise ratio.

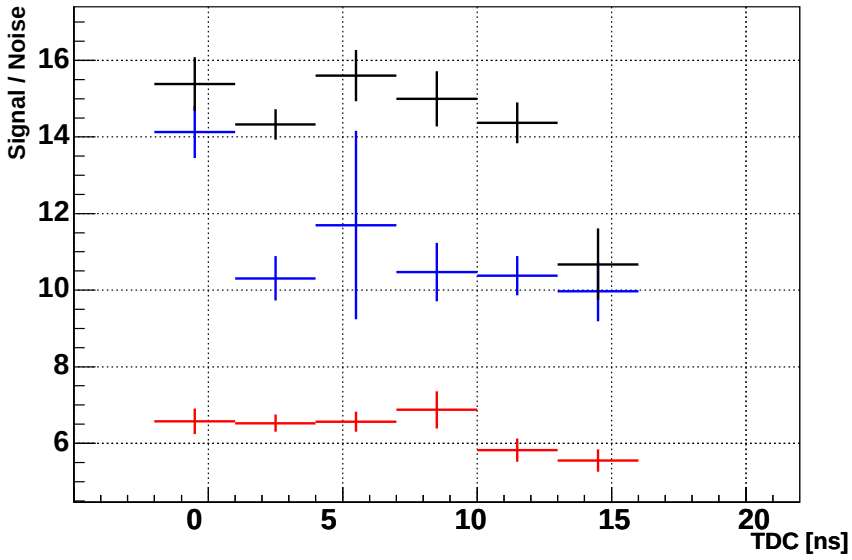

Figure 22: Mean Signal to Noise values measured for an applied bias voltage of 290 V. 7×10^{14} p/cm^2 (red solid points), 4.25×10^{14} p/cm^2 (blue solid points) and 1.25×10^{14} p/cm^2 (black solid points). 290 V is below the depletion voltage.

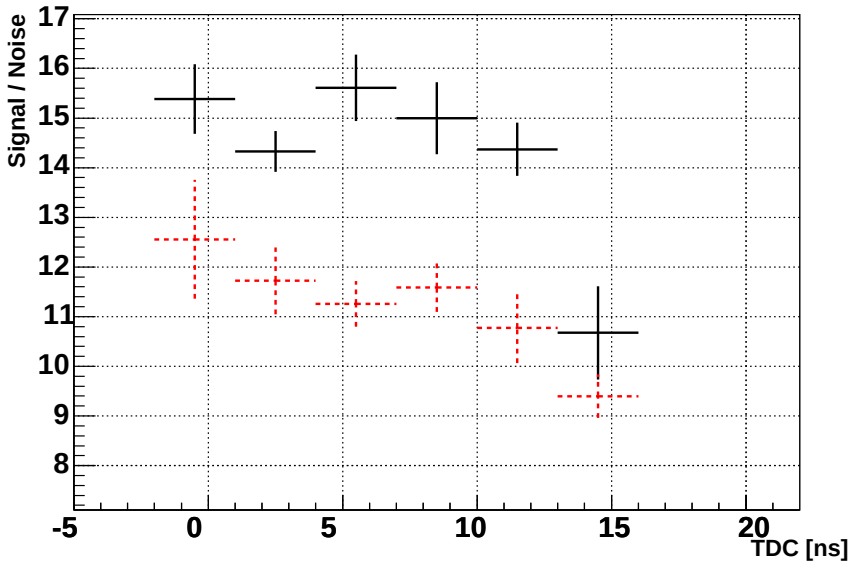

Figure 23: Measured signal to noise ratio for 1.25×10^{14} p/cm^2. 290 V (black solid points) and 243 V (red dashed points).

These studies were the first microstrip detector tests to look into the possibility of using Czochralski silicon for possible LHC upgrades. The detector withstood harsh radiation exposure and showed some promising results. Studies will continue using Cz pad diodes to examine the depletion voltage evolution as a function of radiation.

Acknowledgments

The authors would like to thank the Helsinki Institute of Physics for providing us with the Czochralski detector, in particular Jaakko Haerkoenen. Many thanks to Maurice Glaser, Federico Ravotti for help with the irradiation of the sensor. We would also like to thank Chris Grigson for the use of his colour intensity analysis programme

References

[1] V. Savolainen et al., J. Crystal. Growth, 243, 2, 2003

[2] J. Harkonen et al., Processing of Microstrip Detectors on Czochralski Grown High Resistivity Silicon Substrates, July 2002, submitted to Elsevier Preprint

[3] Radiation Hard Silicon Detectors - Developments by the RD48 (ROSE) Collaboration, Nucl. Instr. & Meth. in Phys. Res. A 466, 308-326, 2001

[4] RD50 Status Report 2002/2003, CERN/LHCC 2003-058

[5] LHCb Vertex Locator Technical Design Report, CERN/LHCC 2001-011

[6] D. Baumeister et al., Characterization of the Beetle-1.0 Front End Chip, LHCb-2001-049

[7] F. Anghinolfi et al.,SCTA - a Rad-Hard BiCMOS Analogue Readout ASIC for the ATLAS Semiconductor Tracker, IEEE Trans. Nucl. Science, 44, No. 3, 1997

[8] J. Libby et al., Measurement of the Irradiation Profile at the PS Beam, LHCb-2001-020

[9] Radiation Damage in Silicon Particle Detectors, M. Moll, DESY-THESIS-1999-040

[10] 3^{RD} RD48 Status Report, F. Lemeilleur *et. al.* CERN/LHCC 2000-009

[11] T. Bowcock et al., Performance of an Irradiated n-on-n Hamamatsu Prototype VELO Detector, LHCb-2001-039

[12] C. Parkes et al., Track Fit - Vertex Locator Test-beam Software Description, LHCb-2001-038

[13] K.S Kölbig and B. Schorr, A program package for the Landau distribution, Computer Phys. Comm. 31 (1984) 97-111